Characterization of the Kinetochore Binding Domain of CENP-E Reveals Interactions with the Kinetochore Proteins CENP-F and hBUBR1

G.K.T. Chan, B.T. Schaar, and T.J. Yen

Institute for Cancer Research, Fox Chase Cancer Center, Philadelphia, Pennsylvania 19111

Abstract. We have identified a 350–amino acid domain in the kinetochore motor CENP-E that specifies kinetochore binding in mitosis but not during interphase. The kinetochore binding domain was used in a yeast two-hybrid screen to isolate interacting proteins that included the kinetochore proteins CENP-E, CENP-F, and hBUBR1, a BUB1-related kinase that was found to be mutated in some colorectal carcinomas (Cahill, D.P., C. Lengauer, J. Yu, G.J. Riggins, J.K. Wilson, S.D. Markowitz, K.W. Kinzler, and B. Vogelstein. 1998. *Nature*. 392:300–303). CENP-F, hBUBR1, and CENP-E assembled onto kinetochores in sequential order during late stages of the cell cycle. These proteins therefore define discrete steps along the kinetochore assembly pathway.

Kinetochores of unaligned chromosome exhibited stronger hBUBR1 and CENP-E staining than those of aligned chromosomes. CENP-E and hBUBR1 remain colocalized at kinetochores until mid-anaphase when hBUBR1 localized to portions of the spindle midzone that did not overlap with CENP-E. As CENP-E and hBUBR1 can coimmunoprecipitate with each other from HeLa cells, they may function as a motor–kinase complex at kinetochores. However, the complex distribution pattern of hBUBR1 suggests that it may regulate multiple functions that include the kinetochore and the spindle midzone.

Key words: kinetochore • mitotic checkpoint • CENP-E • CENP-F • hBubR1 kinase

CHROMOSOME segregation relies on the interactions between microtubules of the spindle and the kinetochore complex, a macromolecular structure that is located at the centromeric heterochromatin of mitotic chromosomes. EM analysis of the kinetochores of mammalian chromosomes show that it appears as a trilaminar disc with approximate dimensions of 80–100-nm thick and between 0.5- and 1.0-μm diam (Rieder, 1982). More recent analysis of the substructure of the trilaminar kinetochore by tomography reveals that each layer has a distinct appearance that may reflect differences in protein composition as well as organization within the kinetochore (McEwen et al., 1993).

The complexity of the kinetochore that was made evident by the ultrastructural studies is supported by the growing list of proteins that reside at the centromere and the kinetochore of mammalian chromosomes. Although the biochemical relationships amongst these proteins within the centromere–kinetochore complex remain undefined, one feature that distinguishes these proteins from one another is their temporal and spatial patterns of distribution (Pluta and Earnshaw, 1995). CENPs A, B, and C were the first human centromere proteins to be identified and are constitutively bound to centromeres throughout the cell cycle (Brenner et al., 1981). All three proteins either interact directly with DNA or are part of the centromeric chromatin. CENP-A is a histone-H3 variant (Sullivan et al., 1994) and has been shown to be localized to a subset of nucleosomes (Palmer et al., 1990). CENP-B is a member of the helix-loop-helix family of DNA binding proteins and recognizes a 17-bp consensus sequence that is found in a subset of alphoid satellite DNA (Muro et al., 1992). Consistent with its DNA binding activity, immuno-EM studies show that CENP-B is localized almost exclusively to the centromeric heterochromatin of mitotic chromosomes (Cooke et al., 1990). CENP-C is a component of the interphase centromere, but during mitosis it is concentrated at the inner kinetochore plate (Saitoh et al., 1992) where it lies in close contact with the centromeric heterochromatin, possibly binding DNA (Sugimoto et al., 1994, 1997; Yang et al., 1996). CENP-G is the most recent member of the constitutive family of centromere proteins that

Address all correspondence to T.J. Yen, Institute for Cancer Research, Fox Chase Cancer Center, 7701 Burholme Ave., Philadelphia, PA 19111. Tel.: (215) 728-2590. Fax: (215) 728-2412. E-mail: TJ_Yen@fccc.edu

localizes to the inner kinetochore plate in mitosis. CENP-G is a 95-kD protein that was identified by an autoimmune serum but its sequence has not been determined (He et al., 1998).

A second group of proteins share the common feature that their appearance at the centromere–kinetochore complex is cell cycle dependent. Careful examination of the localization patterns of the proteins within this group show that they can be distinguished from one another based on the time within the cell cycle that they appear on kinetochores. At present, topoisomerase IIα is the earliest member of this group to appear at the centromere–kinetochores at late S phase (Rattner et al., 1996). This is followed by CENP-F, which is redistributed from the nuclear matrix during early G2 to "pre-kinetochores" by late G2, when chromatin condensation is apparent (Rattner et al., 1993; Liao et al., 1994). By prophase, the nuclear-bound kinesin-related protein MCAK is recruited to the centromere–kinetochore complex (Wordeman, 1995). After nuclear envelope breakdown, hzw10 (Starr et al., 1997) and the molecular motors CENP-E (Yen et al., 1991, 1992) and the dynein–dynactin complex (Pfarr et al., 1990; Steuer et al., 1990; Echeverri et al., 1996), which were in the cytoplasm during interphase, are assembled onto the kinetochore. In addition to the assembly of structural proteins at kinetochores, a group of checkpoint proteins that include hMAD1 (Jin et al., 1998), hMAD2 (Chen et al., 1996; Li and Benezra, 1996), mouse BUB1 (Taylor and McKeon, 1997), and p55cdc (Kallio et al., 1998) assemble onto the kinetochore sometime between prophase and prometaphase. The temporal order of appearance of these proteins at the centromere–kinetochore complex may represent distinct segments of a multi-step pathway for kinetochore assembly. Thus, the mature trilaminar kinetochore that is only visible at mitosis is the end product of a complex assembly pathway that was initiated sometime after replication of the centromeric DNA (He and Brinkley, 1996). To examine this assembly process in greater detail, we have investigated the molecular determinants that specify kinetochore binding by the kinesin-like protein, CENP-E. As CENP-E is detected at all kinetochores by prometaphase, our studies are likely to be focused on one of the final steps in the formation of a fully functional kinetochore. Indeed, immunogold EM data show that CENP-E is concentrated at the fibrous corona (Cooke et al., 1997; Yao et al., 1997), a fibrillar network of proteins that extend away from the outer kinetochore plate.

We localized the kinetochore binding domain in CENP-E by examining the distribution of various fragments of CENP-E that were expressed in transiently transfected mitotic HeLa cells. Using this domain as a bait in a yeast two-hybrid screen, the kinetochore proteins CENP-E, CENP-F, and hBUBR1 were isolated. We show that hBUBR1 assembles onto kinetochores sometime in prophase when CENP-F is already present but before CENP-E has assembled there. As with other checkpoint proteins (Chen et al., 1997; Li and Benezra, 1997; Taylor and McKeon, 1997; Kallio et al., 1998), hBUBR1 and CENP-E staining were stronger on kinetochores of unaligned chromosomes than at kinetochores of aligned chromosomes. In addition to kinetochore localization, hBUBR1 displayed complex distribution pattern from anaphase to telophase. The combined data suggest that hBUBR1 may be a protein kinase that has multiple roles in mitosis that include the kinetochore as well as at the spindle midzone during late anaphase and telophase.

Materials and Methods

Transfection Constructs

All expression constructs used the vector pWS4 that contains the cytomegalovirus (CMV) late promoter and the adenovirus tripartite 5′ UT for efficient initiation of translation (Sheay et al., 1993). This vector was modified to include either the IgG binding domains of protein A (pWSproA), or the green fluorescent protein (pWSgfp). The four IgG binding domains of protein A were amplified by PCR from pRIT2T (Pharmacia Biotech, Inc., Piscataway, NJ) using primers TJY67 (5′-GTATGGAACAACGCATAAC-3′) and TJY68 (5′-GTCTTTAAGGCTTTGGATG-3′). pWS4proA was created by blunt-end ligation of the 775-bp protein A PCR fragment into pWS4 at its NotI site that was blunted by Klenow. The protein A coding region can be released from the vector by BamHI digestion. BamHI sites were added to both ends of the green fluorescent protein (gfp)[1] coding region by PCR from pGFP10.1 (Heim et al., 1995) using primers TJY119 (5′-CGGGATCCATGAGTAAAGGAGAAGA-3′) and TJY156 (5′-GAGGATCCTCTAGAGTATTTGTATAGTTCATCC-3′). The pWS4gfp was made by ligating the 734-bp BamHI gfp fragment into the unique BamHI of pWS4.

CENP-E fusion constructs D, E, F, G, I, J, K, and R were made by directional cloning of BamH- and SalI-digested PCR products into the same sites in pWS4. ProA and/or gfp BamHI cassettes were then ligated into the unique BamHI site of the pWS4–CENP-E constructs. Fragment D was amplified by PCR from pBS/CENP-E (full-length CENP-E cDNA in pBluescript) using primers TJY71 (5′-GTGGATCCCTAGCAACTACACAGTCGA-3′) and TJY103 (5′-ATGTCGACAGTTTTGCACTCAGGCACA-3′). Fragment E was amplified by PCR from pBS/CENP-E using primers TJY71 and TJY74 (5′-ATGTCGACCTTCTCCAAGTCAAGAGAC-3′). Fragment F was amplified by PCR from pBS/CENP-E using primers TJY104 (5′-ATGGATCCAAGGATTCAGCACTACAAAG-3′) and TJY103. Fragment H was amplified by PCR from pBS/CENP-E using primers TJY104 and TJY105 (5′-ATGTCGACCGAGTATTTAACCACTCTTCC-3′). Fragment I was amplified by PCR from pBS/CENP-E using primers TJY71 and TJY108 (5′-ATGTCGACCTCCTTAGCTACAGATTTC-3′). Fragment J was amplified by PCR from pBS/CENP-E using primers TJY102 (5′-ATGGATCCAAGGATTTAGATAAATCAA-3′) and TJY103. Fragment Q was amplified by PCR from pBS/CENP-E using primers TJY149 (5′-TACGGATCCCCTCAGCCTTCAAATAAACC-3′) and TJY103. Fragment B was amplified by PCR from pBS/CENP-E using primers TJY15 (5′-GAATTCATATGGCGGAGGAAGGAGC-3′) and TJY16 (5′-GGATCCTCTAGAGCCTCAAATTC-3′). Expression construct B was made by blunt-end ligation of a blunted NdeI-digested fragment B to blunted ClaI-digested pWS4proA vector. Expression construct C was made by excising a PstI fragment from expression construct B. Construct A was made by directional cloning of a ClaI-cut fragment of CENP-E cDNA 11B into ClaI-digested construct C vector. Construct H was made by excising a EcoRV- and StuI-cut fragment from construct F. Construct K was made by excising a StuI-cut fragment from construct J. Construct L was made by excising a EcoRV- and StuI-cut fragment from construct J. Construct M was made by directional cloning of a XbaI- and SalI-cut fragment of construct J into a XbaI- and SalI-digested pWS4proA vector. Construct N was made by directional cloning of a BamHI and SalI fragment of pSV2-CENP-$E^{COOH368}$ (Liao et al., 1994) into BamHI- and SalI-digested pWS4 vector. Construct O was made by first subcloning a 1.3-kb EcoRI fragment that corresponded to nucleotides 6,469–7,701 of the CENP-E cDNA into EcoRI site of pBluescript (Stratagene, La Jolla, CA). BamHI/SalI digestion of the resultant plasmid released the 1.3-kb CENP-E fragment that was directionally subcloned into BamHI-/SalI-digested pWS4. Construct

1. *Abbreviations used in this paper*: ACA, autoimmune serum containing anti-centromere antibodies; DAPI, 4′,6′-diamino phenylindole; gal, D-galactose; gfp, green fluorescent protein; GST, glutathione-S-transferase; raff, D raffinose.

P was made by deleting the EcoRV and StuI fragment from construct *P* and religating the blunt ends. The gfp-CENP-B expression construct was a gift from K. Sullivan (Scripps Research Institute, La Jolla, CA) (Shelby et al., 1996).

Nuclear targeting constructs (pWS4-NLS) were made by directional cloning of a double-stranded linker (5′-TCGACCAAAAAAGAAGAGAAAGGTAGATCCAAAAAAGAAGAGAAAGTTCGCGA-3′) that encoded two copies of the SV40 T antigen nuclear localization signal, RPKKKRKVDPKKKRKVR (Fischer-Fantuzzi and Vesco, 1988), into the SalI/StuI sites of the pWS4 vector. BamHI/SalI fragments that contained various portions of CENP-E were isolated from the appropriate expression plasmids and inserted into BamHI/SalI sites of pWS4-NLS so that the NLS was fused in the appropriate reading frame of CENP-E.

hBUBR1 expression constructs were made by subcloning PCR products that encoded amino acid residues 1–467, 409–1,051, and 1–1,051 of hBUBR1 into pWSproA and pWSgfp vectors, respectively.

Recombinant Proteins and Antibodies

Affinity-purified rabbit polyclonal anti–CENP-E antibodies HX1 and rat polyclonal anti-gfp antibody were made as described (Schaar et al., 1997). To affinity purify the gfp antibodies, rat sera were adsorbed to an Affigel 10 column that was covalently coupled with maltose binding protein (MBP) to deplete antibodies against MBP. Gfp antibodies were subsequently affinity purified from an Affigel 10 column that was covalently coupled to purified MBP–gfp fusion protein. For production of hBUBR1 antibodies, its COOH-terminal 642 amino acids or NH_2-terminal 350 amino acids were fused to MBP in the pMAL expression vector (New England Biolabs, Beverly, MA) and to glutathione-S-transferase (GST) in pGEX (Pharmacia Biotech, Inc.). Purified MBP fusion proteins were used to immunize rats and rabbits. Antibodies were affinity purified from a column that was coupled with the same segments of hBUBR1 fused to GST. Human autoimmune serum containing anti-centromere antibodies (ACA) was a gift from K. Sullivan. Rabbit polyclonal anti–CENP-F antibodies were made against recombinant CENP-F protein (Liao et al., 1995). Rabbit anti–lex A serum used to examine expression of various lexA:baits was a kind gift of E. Golemis (Fox Chase Cancer Center, Philadelphia, PA).

Transient Transfection and Immunodetection

Monolayers of HeLa cells were grown in DME with 10% FCS at 37°C in 5% CO_2. HeLa cells were transiently transfected by calcium phosphate precipitation (Chen and Okayama, 1987). 36 h after transfection, cells were lysed in NP40 lysis buffer (50 mM Tris-HCl, pH 8.0, 150 mM NaCl, 1% NP40, 1 mM PMSF, and 10 μg/ml protease inhibitors [leupeptin, aprotinin, and pepstatin]), and centrifuged at 16,000 *g* for 15 min at 4°C. ProA-tagged fusion proteins were immunoprecipitated with 25 μl of a 50% slurry of human IgG Sepharose (Pharmacia Biotech, Inc.). Western blots of proA-tagged fusion proteins were incubated with 1:30,000 dilution of alkaline phosphatase–conjugated human IgG (Jackson ImmunoResearch, West Grove, PA). Gfp-CENP-E fusion proteins were detected with rat polyclonal anti-gfp antibody (1:3,000 dilution), followed with alkaline phosphatase–conjugated goat anti–rat secondary antibody (1:30,000 dilution; Sigma Chemical Co.). After extensive washing, filters were processed for chemiluminescence detection according to manufacturer's protocol (Tropix, Bedford, MA).

To localize the distribution of transfected proteins by immunofluorescence, HeLa cells were plated onto coverslips at 40% confluency and transfected by lipofection (LT2; PanVera, Madison, WI). HeLa cells were washed briefly with serum-free OptiMEM (Gibco-BRL, Gaithersburg, MD) and incubated with the DNA–lipid complexes in OptiMEM for 6 h. The lipid–DNA complexes were washed away and replaced with complete medium (DME, 10% FCS). 12–36 h later, transfected cells were extracted in KB (50 mM Tris-HCl, pH 7.4, 150 mM NaCl, 0.1% BSA) with 0.2% Triton X-100 for 5 min at room temperature, washed in KB for 5 min, and then fixed with 3.5% PFA buffered in PBS at pH 6.8 for 10 min. In some cases (indicated in legend), the process was reversed so that samples were fixed and then extracted. Coverslips with proA-CENP-E–transfected cells were incubated with 1:1,000 dilution of Texas red–conjugated human IgG (Jackson ImmunoResearch) in a humidified chamber at 37°C for 15 min. Centromeres were detected by either using a human autoimmune anti-centromere serum (ACA) or by cotransfecting with a CENP-B–gfp construct (Shelby et al., 1996). Microtubules were stained with anti–α-tubulin DM1A mAb (Sigma Chemical Co.). Nuclei and chromosomes were stained with 4′,6′-diamino phenylindole (DAPI). Coverslips were mounted 0.1% *para*-phenylenediamine in glycerol and scanned for transfected cells using a Nikon Microphot SA equipped with epifluorescence optics. Cells were visualized with a 100× Plan Neofluor objective and images were captured with a TEC-1 CCD camera (Dage-MTI, Michigan City, IN) that was controlled with a Macintosh Quadra 650 running IPLab Spectrum (Signal Analytics, Vienna, VA). Image processing was performed using Photoshop 4.0 (Adobe Systems Inc., Mountain View, CA), and figures are composed using Powerpoint 4.0 (Microsoft, Redmond, WA).

Immunoprecipitation was performed by incubating clarified HeLa cell lysates with either CENP-E, CENP-F, or hBUBR1 antibodies for several hours before addition of protein A–Sepharose. Beads were washed five times in cold lysis buffer and separated on a 4–12% denaturing gradient gel. Samples in the gel were transferred onto Immobilon *P* membrane (Millipore Corp., Bedford, MA) and probed with the appropriate antibodies.

Yeast Two-Hybrid Screening

The two-hybrid screen was performed precisely as described (Gyuris et al., 1993; Estojak et al., 1995). The D-galactose (gal)-inducible HeLa cDNA expression library that was cloned in pJG4-5, yeast strains EGY191 and EGY48, as well as yeast expression vectors pEG202, pJG4-5, and pSH18-34 were provided by E. Golemis (Fox Chase Cancer Center). The CENP-E bait containing amino acids 1,958–2,662 was isolated as a BamHI–SalI fragment from pWS4proA:CENP-$E^{1958–2662}$ and inserted into the BamHI–XhoI sites of pEG202 to create a COOH-terminal fusion with amino acids 1–202 of the *lexA* DNA binding domain. The resultant pEG202-CENP-$E^{1958–2662}$ was transformed into EGY191 along with the *lacZ* reporter plasmid pSH18-34. Transformants that did not activate the single-copy *leu2* and the multi-copy *lacZ* reporter genes were then transformed with the HeLa cDNA library. Transformants were selected on ura^-, his^-, and trp^- minimal glucose media to select for the plasmids pEG202-CENP-$E^{1958–2662}$, pSH18-34, and the pJG4-5 library. ura^+, his^+, and trp^+ transformants were harvested from the plates, aliquoted, and then stored at −80°C. 4×10^7 transformants were replated onto ura^-, his^-, trp^-, and leu^- galactose/raffinose (raff) media to select for cDNAs that expressed CENP-E interactors that activated the *leu2* gene. Approximately 500 primary leu^+ colonies were picked and streaked onto X-gal minimal media that contained either glucose or galactose to screen colonies that exhibited gal-dependent activation of the pSH18-34*lacZ* reporter. Approximately 100 colonies that were blue on galactose media but white on glucose media were identified, and the pJG4-5 interactor cDNAs that contained a trp-selectable marker were isolated by transforming trp^- *Escherichia coli* KC8 and selecting for trp prototrophy. In some cases, the cDNA was directly amplified from the yeast mini-prep DNA by PCR using primers that flank the cloning site: EGY175, 5′-CTGAGTGGAGATGCCTCC-3′; RY220, 5′-CTGGCAAGGTAGACAAGCCG-3′. Mini-prep plasmid DNA isolated from *E. coli* KC8, or PCR products were digested with several restriction enzymes and grouped according to their digestion patterns.

Specificity of the interactors were independently verified by retransforming the interactor cDNAs back into EGY191 along with pSH18-34 (*lacZ* reporter) and either pEG202–CENP-$E^{1958–2662}$, or other lexA:baits such as pRFM1 (*Drosophila* bicoid), pEG202-K-rev (gifts of E. Golemis), or pEG202:CENP-$F^{2638–3210}$ (the COOH terminus of CENP-F). cDNAs that only interacted with pEG202–CENP-$E^{1958–2662}$ according to galactose-dependent leu^+/$lacZ^+$ expression were sequenced by an automated sequencer (ABI) using primers EGY175 and RY220.

Mapping the CENP-E That Interact with hBUBR1 and CENP-F

To test for specificity of the interaction between CENP-E and CENP-F, portions of these two cDNAs were subcloned into the appropriate bait or prey vectors. Fragments of CENP-E were isolated from the appropriate pWSproA constructs (see above) as BamHI–SalI fragments that were then ligated into BamHI-/XhoI-digested pEG202 to create in-frame fusions with *lexA*. All of the resultant baits, along with pSH18-34 (*lacZ* reporter) were transformed into EGY48, which contains six *lexO* sites in the promoter of the single copy *leu2* reporter gene. The transformants were verified to not self-activate the reporter genes on galactose media and they were then transformed with pJG–CENP-$F^{1804–2104}$. Four to five colonies from each transformation were restreaked onto minimal ura^-, his^-,

trp⁻, X-gal plates containing glu or gal/raff and also onto minimal ura⁻, his⁻, trp⁻, leu⁻, gal/raff, or glu plates. Plates were incubated at 30°C and inspected 4, 8, 12, and 24 h later for blue color formation on the X-gal plates. Plates were inspected from 18 to 36 h for growth on leu⁻ media. β-galactosidase activity in yeast extracts was quantitated in a liquid assay using ONPG as a substrate (Estojak et al. 1995).

cDNA Cloning and Analysis

The full-length hBUBR1 cDNA was isolated by extending the partial hBUBR1 cDNA that was isolated in the yeast two-hybrid screen towards the 5′ end by RACE (Amplifinder; Clontech, Palo Alto, CA) using TJY300 (5′-GCTGATCACCTGTTCTTTCTTGCTG-3′) as the 3′ primer and nested 5′ primers AP1 and AP2 that were provided in the kit. cDNA template was synthesized from polyA RNA that was isolated from K562 cells. PCR reactions were performed using conditions specified by the manufacturer. The 5′ RACE products were digested with proteinase K (200 μg/ml) for 2–4 h at 37°C, precipitated, gel purified, and then cloned into pGEM-T (Promega, Madison, WI). DNA sequence was determined in both directions with an automated sequencer (PE Applied Biosystems, Foster City, CA). hBUBR1 cDNA was also extended towards its 5′ end by screening a λgt11 human breast carcinoma cDNA library (Clontech) by hybridization. DNA sequence of the phage clones matched and authenticated the RACE products. DNA probes were radiolabeled by random priming and hybridizations were performed in 5×SSPE/5×Denhardt's/0.5% SDS/0.1 mg/ml sheared, sonicated salmon sperm DNA at 60°C. Filters were washed twice with 1×SSC/0.1% SDS at room temperature for 30 min, 0.2×SSC/0.1% SDS between 60°C and 65°C for 10 min, and the filters were exposed to X-ray film. The hBUBR1 sequence data are available from GenBank/DDBJ/EMBL under accession No. AF046918. DNA and protein sequences were analyzed with Wisconsin Package Version 9.1, Genetics Computer Group (Madison, WI), and MacVector 6.0 (Oxford Molecular Biology, Oxford, UK).

Results

Localization of a Kinetochore Binding Domain in CENP-E

The overall strategy to map the kinetochore binding domain of CENP-E was to express various portions of CENP-E in HeLa cells and visualize their distribution by immunofluorescence microscopy. To identify the transfected forms of CENP-E, the fragments were fused in-frame to either the IgG binding domain of protein A (proA), or to the gfp from *Aquaria victoria*. 17 proA–CENP-E fusion constructs that spanned the entire 2,662–amino acid long CENP-E (Fig. 1 *a*) were tested. 10 additional constructs consisting of segments of CENP-E fused to gfp were also tested to independently verify results obtained with the proA–CENP-E constructs. Immunoblot analysis of transfected lysates (Fig. 1 *b*) showed that all 27 constructs expressed proteins of the correct sizes. The presence of two bands in the proA–CENP-E fusions represents the use of an alternative in-frame initiation translation codon within protein A. In all cases, the distribution pattern of each construct was the same regardless of whether it was fused to protein A or gfp.

We predicted that CENP-E would be anchored to the kinetochore near its COOH terminus so that the NH_2-terminal motor domain could extend away from the chromosome to interact with microtubules. We initially focused on analyzing the distribution of the COOH-terminal re-

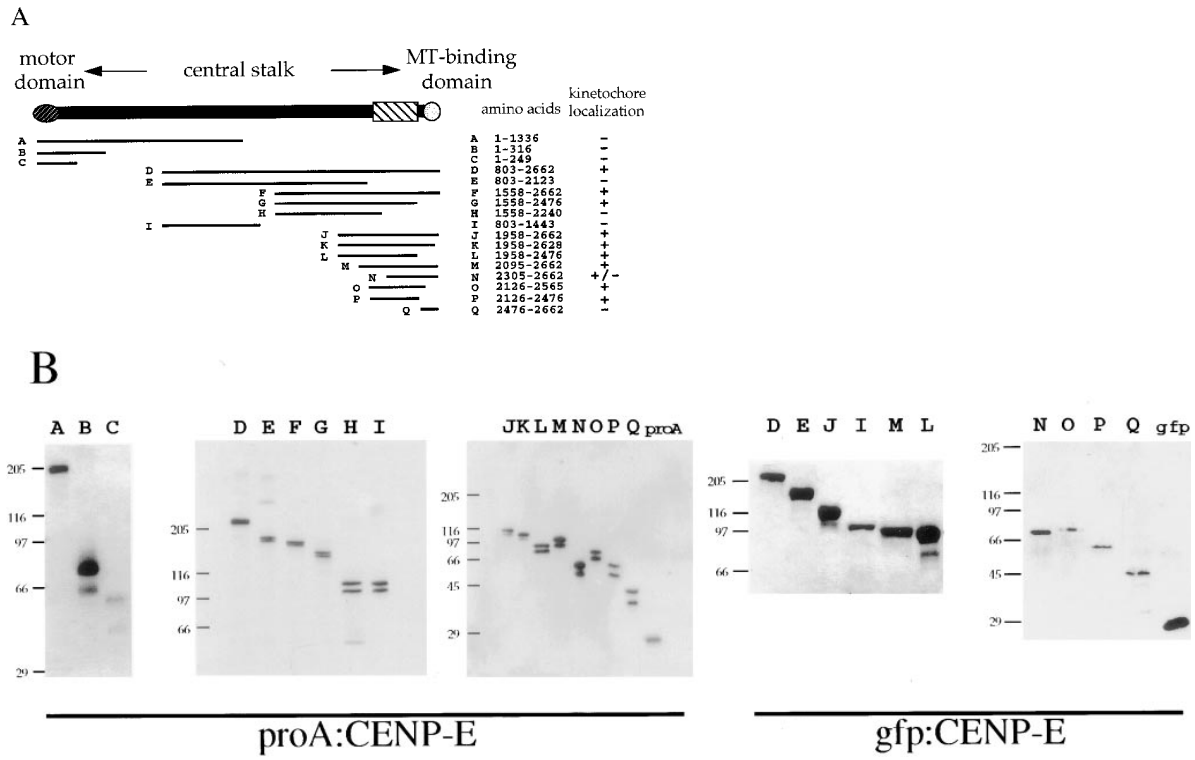

Figure 1. Expression of proA and gfp:CENP-E fusion proteins in HeLa cells. (*A*) Schematic diagram depicting the overlapping set of CENP-E cDNA fragments that were tested for their ability to bind kinetochores (+) or not (−). *Hatched box*, the kinetochore binding domain. (*B*) Immunoblot of transfected cell lysates expressing various proA:CENP-E fusion proteins as detected using alkaline phosphatase–conjugated human IgG. Gfp:CENP-E fusion proteins were detected with rat anti-gfp antibodies.

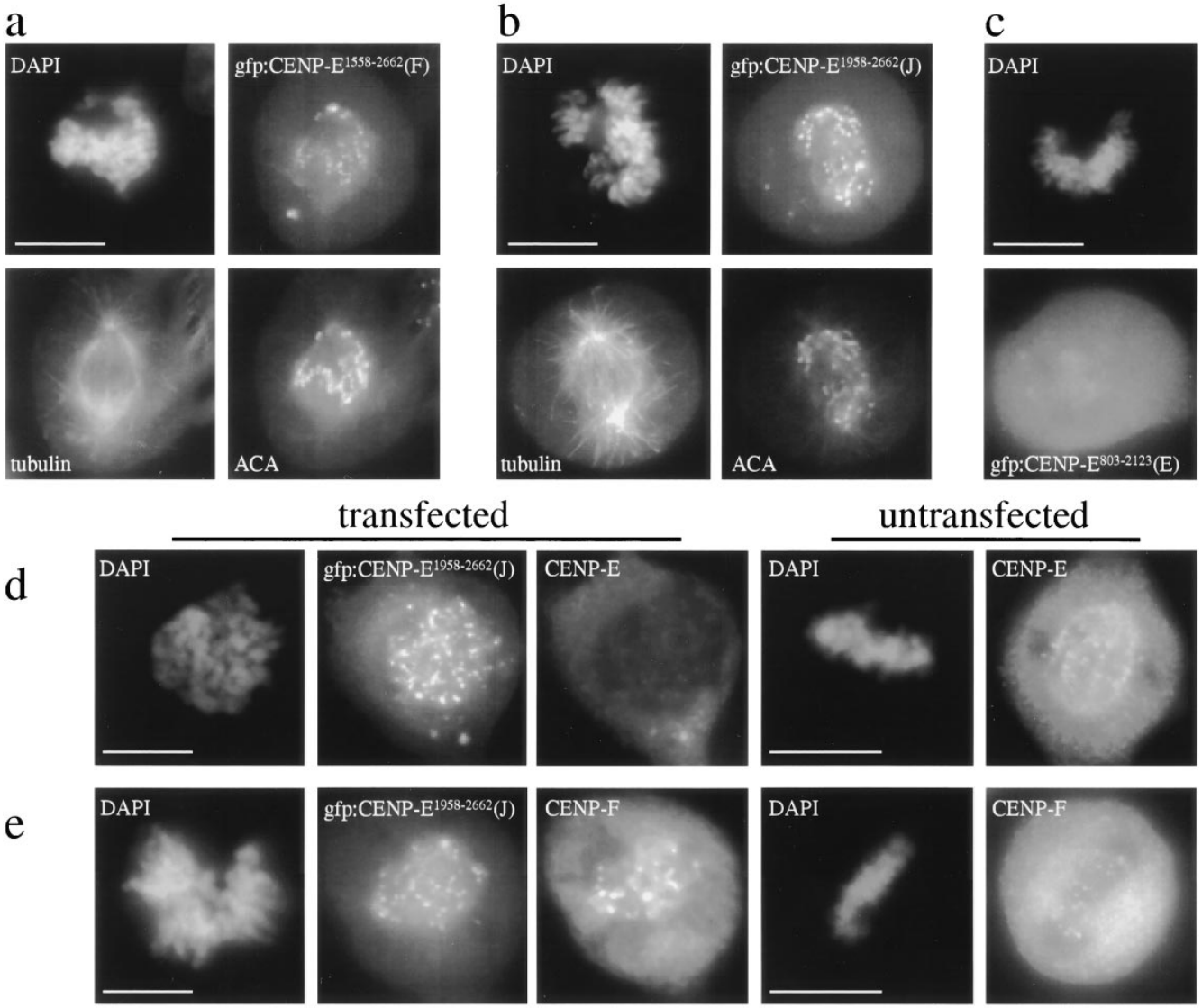

Figure 2. Localization of CENP-E kinetochore binding domain. (*a*) Gfp:CENP-E$^{1558–2662}$(F) binds kinetochores and colocalizes with ACA but not with microtubules. (*b*) Gfp:CENP-E$^{1958–2662}$(J) colocalizes with ACA but not with microtubules. (*c*) Gfp:CENP-E$^{803–2123}$(E) is expressed but not localized to kinetochores. ACA staining was visualized with Cy-5 anti–human secondary antibodies, anti-tubulin antibodies were detected with biotinylated anti–mouse secondary and Texas red conjugated to streptavidin. Gfp fusions were visualized in the FITC channel. (*d*) Kinetochores containing gfp:CENP-E$^{1958–2662}$(J) were probed for endogenous CENP-E using a rabbit anti–CENP-E "neck" antibody (Schaar et al., 1997) and compared with a neighboring untransfected metaphase that was stained with the same antibody. (*e*) Kinetochores containing gfp:CENP-E$^{1958–2662}$(J) probed with CENP-F and compared with an untransfected metaphase cell also probed with CENP-F. Rabbit anti–CENP-E and anti–CENP-F antibodies were detected with Texas red–conjugated anti–rabbit secondary antibodies. Chromosomes were stained with DAPI. All samples were first fixed and then permeabilized. Bars, 10 μm.

gions of CENP-E in transiently transfected HeLa cells. In transfected mitotic cells, gfp:CENP-E$^{1558–2662}$(F) was found to associate at kinetochores as its staining pattern was coincident with ACA staining (Fig. 2 *a*, *top* and *bottom right panels*). Even though this segment of CENP-E contained the COOH-terminal microtubule binding domain, it did not colocalize with microtubules of the spindle (Fig. 2 *a*, *bottom left panel*). This supports our earlier finding that mitotic phosphorylations inhibited microtubule binding by the COOH terminus of CENP-E (Liao et al., 1994). Deletion of the NH_2-terminal 400 residues from gfp:CENP-E$^{1558–2662}$(F) did not affect kinetochore binding as gfp:CENP-E$^{1958–2662}$(J) was prominently detected at kinetochores as confirmed by co-staining with ACA (Fig. 2 *b*, *top* and *bottom right panels*). Other regions of CENP-E that spanned from its NH_2-terminus to residue 2,240 did not contain additional kinetochore binding domains. In all cases where the fusion proteins failed to bind kinetochores in mitosis, immunoblots showed that the overall levels of expression of these constructs were not noticeably different from constructs that bound to kinetochores (Fig. 1 *b*). Immunofluorescence staining revealed that all of these fusion proteins were expressed in mitotic cells but failed to bind kinetochores. As an example, a prometaphase cell

transfected with gfp:CENP-E$^{803–2123}$(E) showed accumulation of gfp fusion protein in the cytoplasm but no kinetochore localization (Fig. 2 *c*, *bottom*).

We have previously shown that gfp:CENP-E$^{803–2662}$(D) competed with endogenous CENP-E for limited binding sites at the kinetochore and disrupted chromosome alignment (Schaar et al., 1997). We therefore examined whether shorter fragments of CENP-E such as gfp:CENP-E$^{1958–2662}$(J) were capable of saturating kinetochores. Using an antibody that was generated against a portion of CENP-E that was absent in the transfected construct, kinetochores that contained gfp:CENP-E$^{1958–2662}$(J) did not exhibit detectable levels of endogenous CENP-E (Fig. 2 *d*, *middle* and *right panels* of transfected cell). This antibody was clearly able to identify CENP-E at the kinetochores of an untransfected metaphase cell that was on the same coverslip (Fig. 2 *d*, *untransfected panel*). This finding showed that kinetochore binding by the transfected CENP-E fragments was not achieved by binding to endogenous CENP-E but was mediated through interactions with other kinetochore proteins. On the other hand, kinetochores saturated with gfp:CENP-E$^{1958–2662}$(J) did not affect the kinetochore localization of CENP-F (Fig. 2 *e*, *right*, *transfected panel*) as its staining intensity was comparable to a neighboring untransfected metaphase cell (Fig. 2 *e*, *untransfected panel*).

One of the consequences of depleting endogenous CENP-E from kinetochores by overexpression of the kinetochore binding domain of CENP-E was that chromosomes failed to align at the spindle equator. As bipolar spindle formation appeared normal in these cells (Fig. 2, *a* and *b*, *bottom left panels*), disruption of chromosome must be due to defective kinetochore functions. These data are entirely consistent with our earlier finding that chromosome alignment was disrupted when kinetochores were either depleted of CENP-E or saturated with a motorless CENP-E mutant (Schaar et al., 1997).

Analysis of additional deletion constructs showed that CENP-E$^{2095–2662}$(M) retained an intact kinetochore binding domain (data not shown). Interestingly, deleting 210 residues from NH_2 terminus of CENP-E$^{2095–2662}$ did not abolish kinetochore binding activity but affected binding in a qualitative way. Unlike the larger fragments that were invariably bound to kinetochores, CENP-E$^{2305–2662}$(N) was not consistently found at kinetochores of all transfected mitotic cells. On the same coverslip, we found transfected mitotic cells whose kinetochores contained CENP-E$^{2305–2662}$(N) (Fig. 3 *b*) as well as mitotic cells that expressed this protein but showed staining on only a few chromosomes (Fig. 3 *d*). The variability in kinetochore binding by CENP-E$^{2305–2662}$(N) was unlikely to be due to cell to cell variation in its expression level as such variability was not seen for the other 15 constructs that expressed the kinetochore binding domain. The variable kinetochore binding activity is also unlikely to be due to differences between prometaphase versus metaphase as other constructs did not exhibit mitotic stage dependent kinetochore binding (e.g., compare Fig. 2, *a* and *b*). This data suggested that elements between residues 2,095 and 2,305 were necessary to achieve efficient and stable kinetochore binding activity. To delineate boundaries of the targeting domain further, the NH_2 and COOH termini of CENP-E$^{2095–2662}$(M) were deleted. The resultant construct, CENP-E$^{2126–2476}$(P) was found to bind kinetochores in all transfected mitotic cells (Fig. 3 *f*). The combined transfection data show that the minimal kinetochore binding domain resided between residues 2,126 and 2,476 of CENP-E and did not overlap the adjacent COOH-terminal microtubule binding domain (Liao et al., 1994).

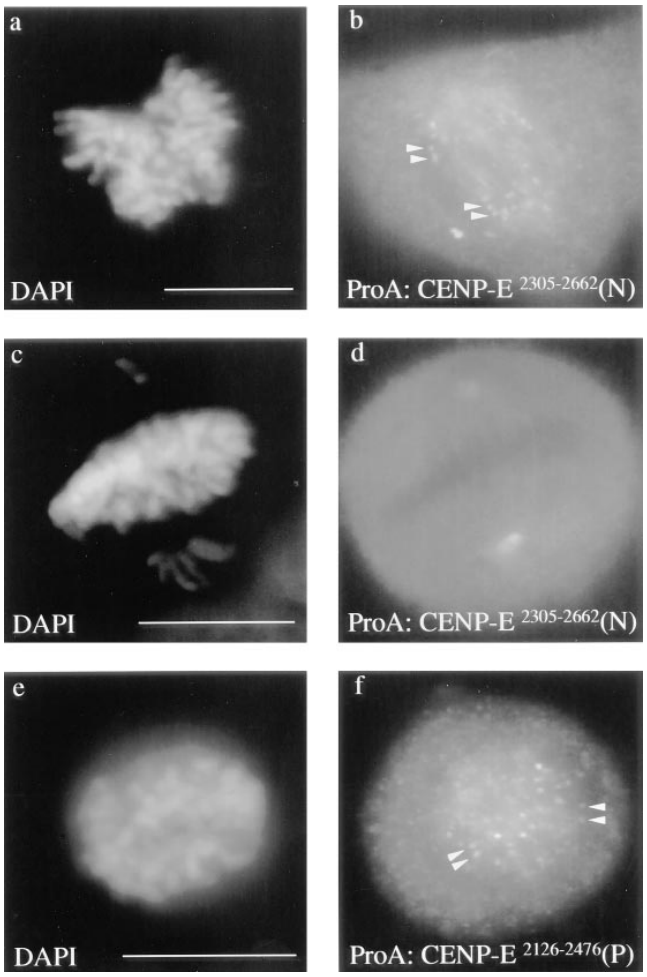

Figure 3. Localization of the minimal kinetochore binding domain. proA:CENP-E$^{2305–2662}$(N) binds to all kinetochores in one cell (*b*) but only a few in another (*d*). (*f*) The minimal kinetochore binding domain lies within proA:CENP-E$^{2126–2476}$(P). ProA:CENP-E fusions were visualized with Texas red conjugated to human IgG (*b*, *d*, and *f*). Chromosomes are stained with DAPI (*a*, *c*, and *e*). *Arrowheads*, double-dot kinetochore staining. All samples were first fixed and then permeabilized. Bars, 10 μm.

Kinetochore Binding by CENP-E Is Restricted to Mitosis

Human CENP-E is detectable only in the cytoplasm of interphase cells (Yen et al., 1992), whereas *Xenopus* CENP-E was found to be a nuclear protein (Wood et al., 1997). In both cases, kinetochore localization is first detected very early in mitosis. To directly test whether human CENP-E is capable of interacting with kinetochore or centromeric components before mitosis, the kinetochore binding domain of CENP-E was ectopically expressed in interphase

nuclei. Targeted expression in nuclei was accomplished by fusing two copies of the SV40 T Ag nuclear localization sequence at the COOH terminus of proA:CENP-E$^{2126–2565}$(O) fusions that displayed kinetochore binding. Western blots confirmed the protein was properly expressed (Fig. 4 *a*). As the IgG binding domain was fused to CENP-E, we were unable to use ACA to stain centromeres. We therefore cotransfected cells with a CENP-B:gfp construct that allowed direct comparison of the distribution of proA:CENP-E$^{2126–2565}$:NLS(O) and the centromere-bound CENP-B:gfp. Examination of transfected interphase HeLa cells showed that proA:CENP-E$^{2126–2565}$:NLS(O) accumulated in nuclei but failed to colocalize with centromeres that were identified by CENP-B:gfp (Fig. 4 *d*). Instead, the proA:CENP-E$^{2126–2565}$:NLS(O) fusion protein was concentrated at the periphery of nucleoli or formed small granules that might be protein aggregates (Fig. 4 *c*). When other portions of CENP-E that did not contain the kinetochore binding domain were expressed in the nucleus, they displayed a uniform distribution pattern that excluded nucleoli (data not shown). The inability of the kinetochore binding domain of CENP-E to bind to interphase centromeres was unlikely due to interference by the NLS. This was made evident when proA:CENP-E$^{2126–2565}$:NLS(O) was detected at kinetochores of transfected mitotic cells (Fig. 4 *f*).

Identification of Kinetochore Proteins That Bind to CENP-E

To search for proteins that associate with the kinetochore binding domain of CENP-E, CENP-E$^{1958–2662}$(J) was used to screen a galactose-inducible HeLa cDNA expression library by the yeast two-hybrid approach. To increase the stringency of the screen, we chose a host that contained only two *lexO* sites within the promoter of the single-copy *leu2* reporter gene. In principle, transcriptional activation of this promoter requires that the interactor that is fused to the transactivation domain to exhibit a higher affinity for the bait than a situation where the promoter has additional *lexO* sites that can accommodate additional molecules of bait. Of the ~500 primary leu$^+$ colonies that were isolated in the presence of galactose, ~100 were found to also activate the multi-copy *lacZ* reporter plasmid in the presence of galactose but not glucose. The interactor cDNAs were isolated and re-transformed into the same host to independently confirm their interaction with CENP-E. In addition, the interactors were tested against several unrelated baits such as, *bicoid*, and K-rev, to eliminate interactors that exhibited promiscuous associations. The DNA sequence of the interactors that specifically interacted with CENP-E were then determined.

Four cDNAs that were isolated multiple times (>6) encoded portions of ferritin, cytokeratin, the kinetochore protein CENP-F, and a kinase that was identical to hBUBR1 (see below). Ferritin and cytokeratin interactors were likely false-positives. The CENP-F interactor encoded residues 1,804–2,104 that were derived from the middle of the 3,210-residue protein. The BUB1-like kinase interactor consisted of its COOH-terminal 641 residues. A second group of interactors were isolated at a lower frequency (<3). The difference in the frequency may simply reflect the relative abundance of these cDNAs in the library as opposed to differences in the specificity of the individual interactors per se. Two interactors were novel proteins with no strong sequence homology with other proteins in the database and they have not been further characterized. The third interactor (isolated twice) within this group encoded amino acids 1,989–2,353 of CENP-E. As this portion of CENP-E lies within the CENP-E$^{1958–$

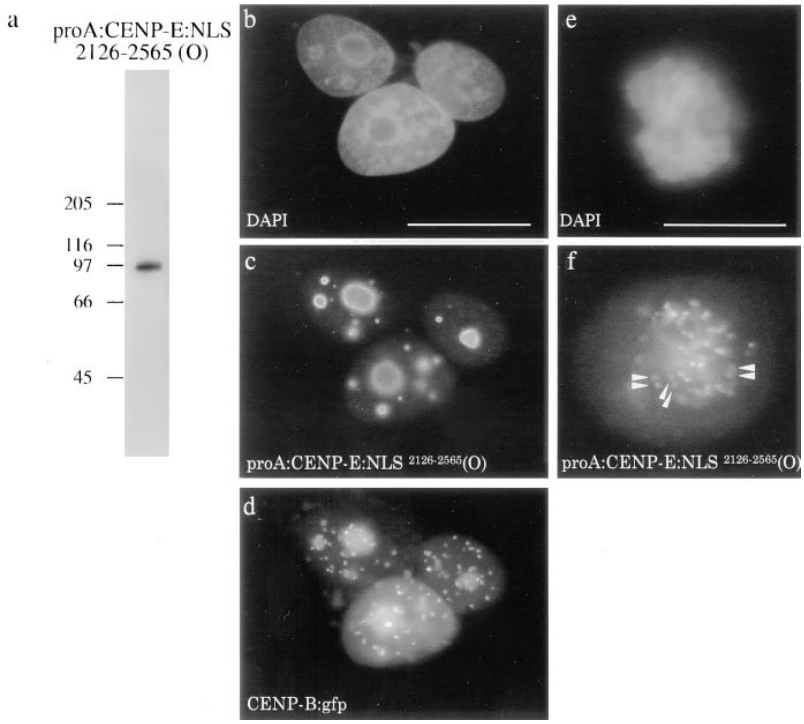

Figure 4. Ectopic expression of CENP-E in interphase nuclei. (*a*) HeLa lysates express proA:CENP-E$^{2126–2565}$:NLS(O). Immunoblot was probed with alkaline phosphatase–conjugated human IgG. (*b–d*) HeLa cells cotransfected with (*c*) proA:CENP-E$^{2126–2565}$:NLS(O) and (*d*) CENP-B:gfp. (*e* and *f*) ProA:CENP-E$^{2126–2565}$:NLS(O) localize to kinetochores during mitosis. (*c* and *f*) ProA:CENP-E$^{2126–2565}$:NLS(O) was visualized with Texas red–conjugated human IgG. (*b* and *e*) Chromosomes and nuclei were visualized with DAPI. *Arrowheads*, double-dot kinetochore staining. All samples were first fixed and then permeabilized. Bars, 10 μm.

^{2662}(J) bait, elements within this region must specify self-association. This is consistent with the possibility that native CENP-E may exist as a homodimer (Thrower et al., 1995).

Examination of CENP-E and CENP-F Interactions

As CENP-F is a nuclear matrix protein during most of interphase whereas CENP-E is mostly cytoplasmic, we tested whether a stable CENP-E and CENP-F complex was formed during mitosis when both proteins are present in the same compartment. Using various lysis conditions, we failed to detect CENP-E in CENP-F immunoprecipitates and vice versa. Likewise, CENP-E$^{1958–2662}$ and CENP-F$^{1804–2104}$ that were purified from bacteria or expressed in a reticulocyte lysate failed to form complexes in vitro. As both the CENP-E bait and the CENP-F interactor were predicted to form extensive coiled-coil interactions, we wanted to verify that these interactions were not simply due to non-specific coiled-coil interactions. We therefore tested CENP-F$^{1804–2104}$ for its ability to interact with CENP-E$^{1558–2240}$(H) and CENP-E$^{803–1443}$(I), two segments that were predicted to contain extensive coiled-coil domains but did not share extensive overlap with CENP-E$^{1958–2662}$(J). We also tested whether the CENP-F$^{1804–2104}$ was capable of interacting with the coiled-coil domains that were predicted to be present in another portion of CENP-F such as its COOH-terminal 572 amino acids. Despite the fact that we used a *lacZ* reporter that contained six *lexO* sites and is thus sensitive to weak protein interactions, no β-galactosidase activity was detected between these segments of CENP-E and CENP-F (Table I).

We attempted to localize the portion of CENP-E$^{1958–2662}$(J) that specified interactions with CENP-F$^{1804–2104}$ by using the yeast two-hybrid assay. Comparison of the β-galactosidase activities obtained with each combination of bait and prey showed that only CENP-E$^{1958–2662}$(J) and CENP-E$^{2095–2662}$(M) interacted with CENP-F. CENP-E$^{2095–2662}$(O) and CENP-E$^{2126–2565}$(P) did not interact with CENP-F even though they associated with kinetochores in vivo (Table I). Western blots confirmed that all lexA: CENP-E fusion proteins were expressed at comparable levels thus eliminating the possibility that the lack of reporter activity was due to instability of the bait (data not shown).

Isolation of hBUBR1 Kinase

One of the interactors that we isolated contained a conserved kinase domain (Hanks and Quinn, 1991; Hanks and Hunter, 1995). When the cDNA was extended towards its 5′ end, it was found to encode a protein that exhibited 15% identity, 30% similarity with the yeast BUB1 spindle checkpoint kinase (Hoyt et al., 1991), and 21% identity, 37% similarity with the mouse BUB1 checkpoint kinase (Taylor and McKeon, 1997). During the course of our work, Cahill and co-workers (1998) isolated hBUB1 and hBUBR1, two human BUB1-like kinases that were mutated in some colorectal carcinomas. Comparison of the sequences of hBUB1, hBUBR1, and our kinase showed that we had isolated hBUBR1. A dendrogram depicting the relatedness of the human, rat, mouse, and yeast BUB1 kinases show that hBUB1 is the homologue of mouse BUB1. A partial rat cDNA (these sequence data are available from GenBank/EMBL/DDBJ under accession No. U83666) that encoded 165 amino acids was found to be most homologous with residues 127–292 of hBUBR1 and is thus likely to be the rat BUBR1 homologue (Fig. 5 *a*).

As was first reported for yeast BUB1 (Roberts et al., 1994), the NH_2-terminal portion of all mammalian BUB1 kinases shared extensive homology with a portion of the yeast checkpoint protein, MAD3p (Li and Murray, 1991; direct submission GenBank accession No. 1006729). Alignment of these sequences showed there are blocks of conserved residues throughout this domain (Fig. 5 *b*). Within this region, yeast BUB1 and hBUBR1 exhibited 44% identity and 66% similarity, and 37% identity and 68% similarity, respectively, with MAD3. Mouse and human BUB1 were 25% identical and 45–47% similar to MAD3. The homology scores between the MAD3-like domain of hBUBR1 and yeast BUB1 is much greater than the 15% identity and 30% similarity that they share throughout their entire lengths. As a result of the strong similarity shared between this portion of hBUBR1 and yeast MAD3, a search for the human MAD3 homologue led to the independent isolation of hBUBR1 (Taylor et al., 1998). However, hBUBR1 does not appear to be the human MAD3 homologue because it contains a kinase domain that is not present in yeast MAD3.

To characterize hBUBR1 in greater detail, affinity-purified antibodies specific to hBUBR1 were isolated. In addition, we generated antibodies specific to hBUB1 as this kinase was isolated in a separate yeast two-hybrid screen that was designed to isolate proteins that interacted with the kinetochore targeting domain of CENP-F (Yen, T.J., unpublished results). We relied on the size difference between hBUB1 and hBUBR1 to confirm the specificity of the hBUBR1 antibodies. Consistent with the fact that the calculated mass of hBUB1 is ~10-kD greater than hBUBR1, hBUBR1 antibodies identified a single protein in HeLa lysates that was smaller than the one identified by hBUB1 antibodies (Fig. 5 *c*, compare lanes *1* and *2*). To eliminate lane to lane variances, a filter probed with hBUB1 was stripped and reprobed with hBUBR1 antibodies to show that the difference in size between these two proteins could be resolved by SDS-PAGE (Fig. 5 *c*, lanes *3* and *4*).

hBUBR1 Exhibits a Complex Distribution Pattern

Examination of the subcellular distribution of hBUBR1 by immunofluorescence staining showed that it was con-

Table I.

Bait	Prey CENP-F$^{1804–2124}$
CENP-E$^{1558–2240}$(H)	12 ± 4*
CENP-E$^{803–1443}$(I)	8 ± 2
CENP-F$^{2638–3210}$	12 ± 4
CENP-E$^{1958–2662}$(J)	841 ± 84
CENP-E$^{2095–2662}$(M)	1,237 ± 63
CENP-E$^{2126–2565}$(O)	17 ± 9
CENP-E$^{2126–2476}$(P)	15 ± 1

*β-Galactosidase units averaged from three independent assays.

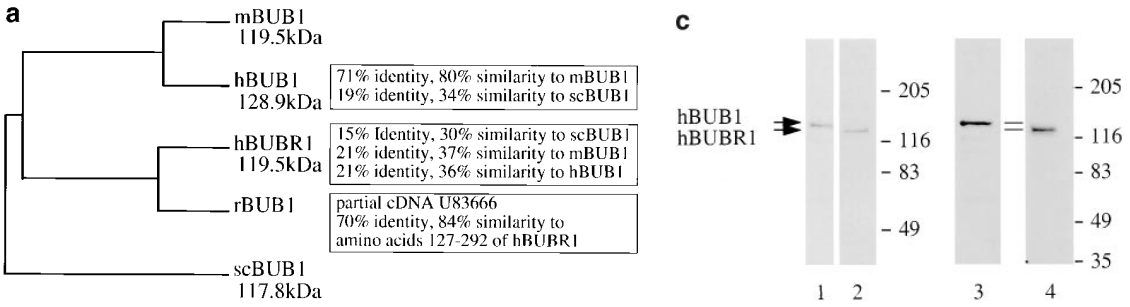

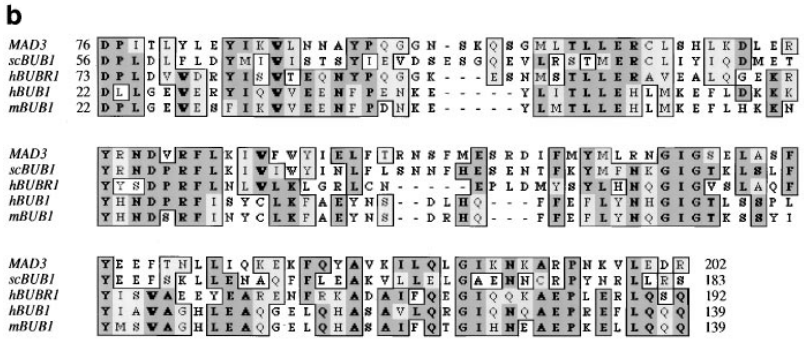

Figure 5. Identification of human hBUBR1 kinase. (*a*) Dendrogram depicting the relatedness of yeast, mouse, rat (partial clone), and human BUB1 kinases was generated with GCG PILEUP program. (*b*) Alignment of the NH_2-terminal portion of mBUB1, hBUBR1, yeast BUB1, and yeast MAD3. Identical and conserved residues in boxed region are bolded and shaded, respectively. Alignment was performed with ClustalW in MacVector 6.0.1. (*c*) 50 μg of HeLa lysate was probed with affinity-purified hBUBR1 antibodies (lanes *2* and *4*) and affinity-purified hBUB1 antibodies (lane *1* and *3*). A filter probed with hBUB1 antibodies (lane *3*) was stripped and re-probed with hBUBR1 antibodies (lane *4*), to show that hBUB1 and hBUBR1 can be resolved from each other. The bars show the separation of the two bands if lanes *3* and *4* were superimposed.

centrated in the cytoplasm of all interphase cells (Fig. 6, *a* and *b*). The cytoplasmic staining of hBUBR1 in both interphase and mitotic cells was reduced significantly if cells were pre-extracted with a mild detergent (data not shown). Kinetochore localization of hBUBR1 was first detected in early prophase, before CENP-E was detected there (Fig. 6, compare *d* and *e*). Although this pattern was only seen a few times (<10) on each coverslip, it was consistently found from experiment to experiment. The earliest time that CENP-E was detected at kinetochores was in very early prometaphase (Fig. 6 *h*). At this cell cycle stage, not all kinetochores that were occupied by hBUBR1 were

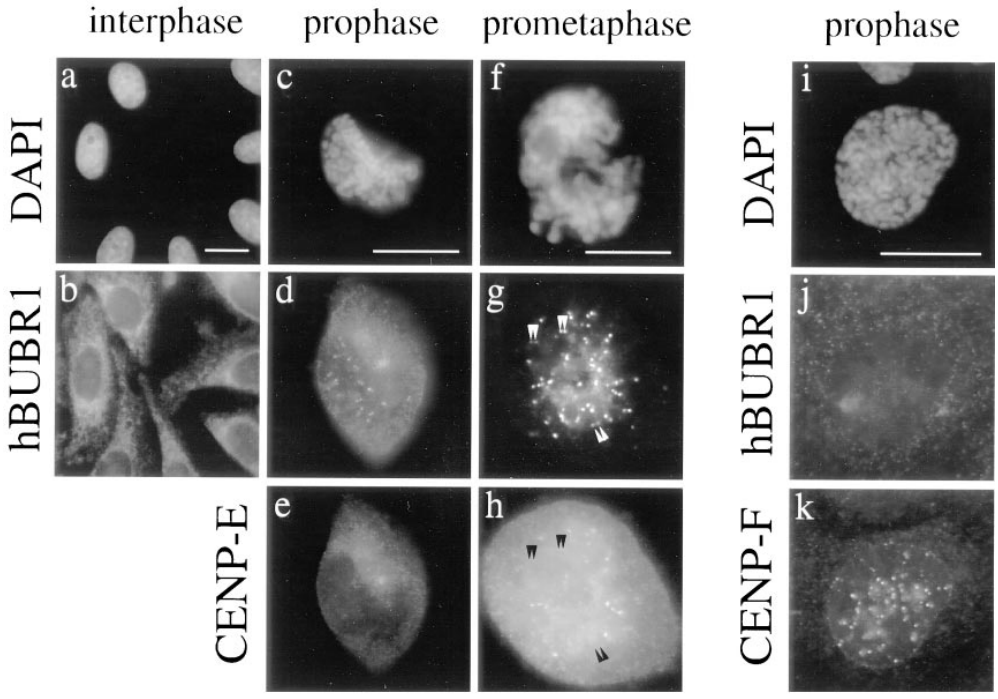

Figure 6. hBUBR1 assembles on kinetochores after CENP-F but before CENP-E. (*b*) hBUBR1 distribution in interphase HeLa cells. (*c–h*) Double staining of a prophase and early prometaphase cell with hBUBR1 and CENP-E. Arrowheads point to kinetochores that contain hBUBR1 (*g*) but not CENP-E (*h*). (*i–k*) Double staining of a prophase cell with hBUBR1 and CENP-F. In *c–e* and *i–k*, cells were extracted before fixing to reduce soluble pools of proteins that would obscure detection of kinetochore staining. hBUBR1 (*b*, *d*, *g*, and *j*) was stained with rat anti-hBUBR1 antibodies and Cy2–anti-rat IgG. CENP-E (*e*, *h*) and CENP-F (*k*) were stained with rabbit anti–CENP-E and CENP-F antibodies, respectively, and counterstained with Texas red–anti-rabbit IgG. Chromosomes and nuclei were stained with DAPI (*a*, *c*, *f*, and *i*). *a* and *b* were photographed with a 40× objective while other panels were photographed with a 100× objective. Bars, 10 μm.

found to contain CENP-E as the staining intensity of CENP-E varied amongst the kinetochores that exhibited hBUBR1 staining (Fig. 6, *g* and *h*). To further narrow the time-frame when hBUBR1 assembled onto kinetochores, we compared its staining pattern to that of CENP-F which also assembles onto kinetochores before CENP-E (Liao et al., 1995). Reproducibly, we found a small number of late G2 to prophase cells (~5 per coverslip) whose kinetochores contained CENP-F but not hBUBR1. The example shown in Fig. 6, *i–k* is a prophase cell that exhibited CENP-F staining at kinetochores but not hBUBR1. The combined data show that hBUBR1 assembled onto kinetochores sometime in prophase, after CENP-F but before CENP-E.

During prometaphase, CENP-E and hBUBR1 colocalized at kinetochores (Fig. 7, *a–c*). In all cases examined, kinetochores of unaligned chromosomes exhibited stronger hBUBR1 and CENP-E staining than at kinetochores of aligned chromosomes. In one of the more dramatic examples (Fig. 7, *d–f*, *insets*), we observed a cell in which the trailing kinetochore of a congressing chromosome exhibited brighter hBUBR1 and CENP-E staining than its leading sister kinetochore or other kinetochores that were aligned. By mid-anaphase, kinetochores exhibited weak hBUBR1 and CENP-E staining (Fig. 7, *g–i*). At this time however, hBUBR1 was diffusely distributed throughout the spindle (Fig. 7 *h*) but did not colocalize with CENP-E that was concentrated at the spindle midzone (Fig. 7 *l*). By late anaphase, hBUBR1 was prominently distributed in two patches in the spindle midzone that flanked a narrow stripe of CENP-E (Fig. 7, *k* and *l*). By telophase, the patches of hBUBR1 staining gave way to a granular staining pattern that was diffusely distributed throughout the dividing cell (Fig. 7 *n*). CENP-E on the other hand was prominently concentrated at the midbody (Fig. 7 *o*).

hBUBR1 Forms a Complex with CENP-E in HeLa Cells

To verify the interaction between hBUBR1 and CENP-E that was detected using the yeast two-hybrid assay, we examined whether hBUBR1 and CENP-E formed a complex in HeLa cells. Lysates from asynchronous HeLa cells were incubated with either CENP-E or hBUBR1 antibodies and the immunoprecipitates were examined for the presence of coprecipitating hBUBR1 or CENP-E (Fig. 8 *a*). Immunoprecipitates obtained with hBUBR1 antibodies were found to contain hBUBR1 (Fig. 8 *a*, *bottom panel* of lane *1*) as well as coprecipitating CENP-E (Fig. 8 *a*, *top panel* of lane *1*). Consistent with these results, a CENP-E

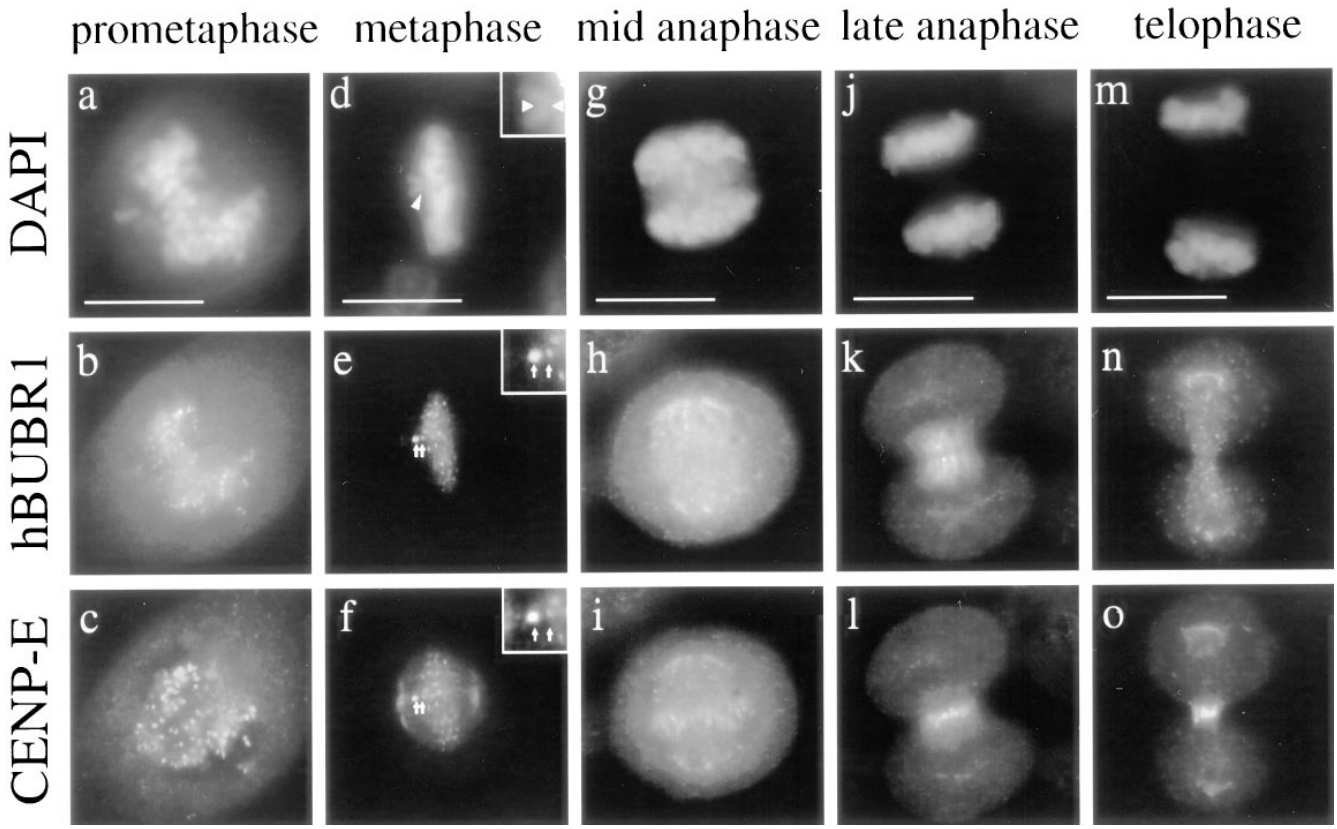

Figure 7. hBUBR1 and CENP-E exhibit complex localization patterns during mitosis. Double-immunofluorescence staining of hBUBR1 (*b*, *e*, *h*, *k*, *n*) and CENP-E (*c*, *f*, *i*, *l*, *o*) of cells from prometaphase to telophase. The *inset* in *d*, depicts a single unaligned chromosome. Left and right arrowheads point to trailing and leading kinetochores, respectively. The trailing kinetochore exhibits stronger hBUBR1 (*e*) and CENP-E (*f*) staining than its leading kinetochore. All samples were extracted and then fixed to reduce staining contributed by the soluble pools of hBUBR1 and CENP-E. Identical antibodies were used as in Fig. 6. Bars, 10 μm.

immunoprecipitate was found to contain hBUBR1 (Fig. 8 *a*, lane *2* [The smaller fragments correspond to hBUBR1 degradation products.]). In contrast, nonimmune antibodies that did not contain CENP-E antibodies failed to immunoprecipitate CENP-E or hBUBR1 (Fig. 8 *a*, lane *3*).

To localize the domain within hBUBR1 that mediated the interaction with CENP-E, the NH_2- and COOH-terminal halves of hBUBR1 were expressed as proA fusion proteins in transiently transfected HeLa cells (Fig. 8 *b*). Immunoprecipitates containing the proA:hBUBR1$^{1–467}$ and proA:hBUBR1$^{409–1051}$ were then probed for the presence of endogenous CENP-E. Consistent with the yeast two-hybrid data, the COOH-terminal 642 amino acids of hBUBR1 was found to associate with CENP-E (Fig. 8 *b*, lane *1*) while no interaction was detected between CENP-E and the NH_2-terminal 467 residues of hBUBR1 (Fig. 8 *b*, lane *2*). To eliminate the possibility that CENP-E binding resulted from an artifact created by the proA:hBUBR1 fusion, we demonstrate that endogenous CENP-E can also associate with gfp:hBUBR1$^{1–1051}$ but not gfp alone (Fig. 8 *b*, lanes *3* and *4*).

To verify that the kinetochore binding domain of CENP-E mediated the interaction with hBUBR1, HeLa cells were cotransfected with gfp:CENP-E$^{1958–2662}$(J) and either proA:hBUBR1$^{1–467}$ or proA:hBUBR1$^{409–1051}$. When immunoprecipitates containing the two different proA: hBUBR1 fusion proteins (Fig. 8 *b*, lane *5* and *6*) were probed with gfp antibodies, the gfp:CENP-E$^{1958–2662}$(J) was found to coprecipitate with proA:hBUBR1$^{409–1051}$ (Fig. 8 *b*, lane *5*). Western blot analysis of lysates obtained from cells that were cotransfected with these constructs showed that gfp:CENP-E$^{1958–2662}$ was expressed along with proA: hBUBR1$^{1–467}$ (Fig. 8 *b*, lane *7*) and proA:hBUBR1$^{409–1051}$ (Fig. 8 *b*, lane *8*). The interaction between proA: hBUBR1$^{409–1051}$ and gfp:CENP-E$^{1958–2662}$ is mediated through the CENP-E portion of the gfp:CENP-E hybrid as gfp alone failed to associate with proA:hBUBR1$^{409–1051}$ (data not shown).

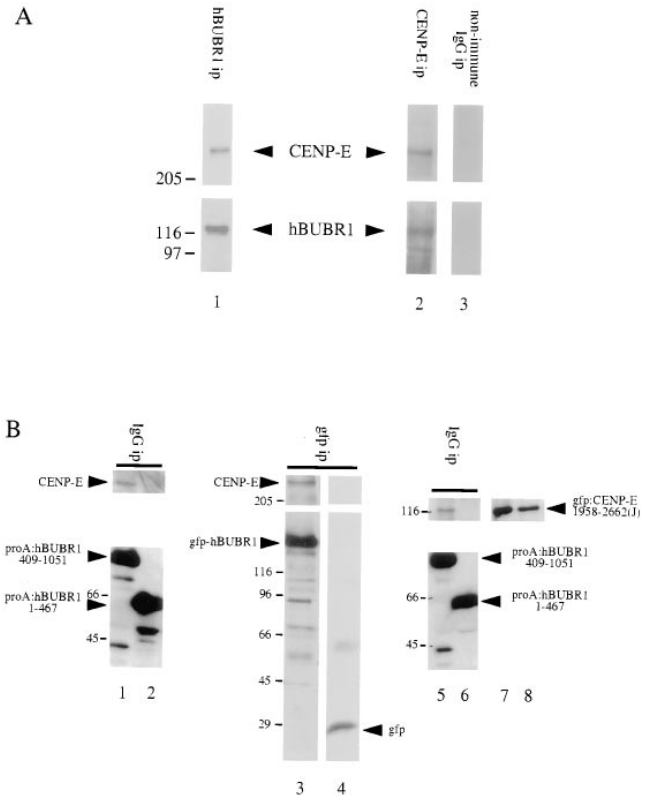

Figure 8. hBUBR1 forms a complex with CENP-E in HeLa cells. (*a*) Affinity-purified rat anti-hBUBR1 IgG was used to immunoprecipitate hBUBR1, and then probed with rabbit anti-hBUBR1 (*bottom panel*, lane *1*) and rabbit anti–CENP-E antibodies (*top panel*, lane *1*). Immunoprecipitates obtained with CENP-E antibodies (lane *2*) and nonimmune antibodies (lane *3*) were probed with CENP-E (*top panel*) and hBUBR1 (*bottom panel*). The filter was cut and the appropriate sections were probed with hBUBR1 and CENP-E antibodies. (*b*) ProA:hBUBR1$^{409–1051}$ (lane *1*), proA:hBUBR1$^{1–467}$ (lane *2*), gfp:hBUBR1 (lane *3*), and gfp (lane *4*) were immunoprecipitated from transfected lysates with human IgG Sepharose and anti-gfp antibodies, respectively, and probed for coprecipitating CENP-E (lanes *1–4*, *top panels*). Lysate prepared from cells cotransfected with gfp:CENP-E$^{1958–2662}$ and proA:hBUBR1$^{409–1051}$ (lane *5*) or proA:hBUBR1$^{1–429}$ (lane *6*) were incubated with human IgG Sepharose to immunoprecipitate the proA:CENP-E fusion proteins (lanes *5* and *6*, *bottom panel*), and then probed for coprecipitating gfp:CENP-E$^{1958–2662}$ (*top panel*). Expression of gfp:CENP-E$^{1958–2662}$ in cells cotransfected with either proA:hBUBR1$^{409–1051}$ (see lane *7*) or proA:hBUBR1$^{1–467}$ (see lane *8*) was confirmed by Western blot. ProA:CENP-E and gfp:CENP-E fusions were detected with alkaline phosphatase–conjugated human IgG and rat anti-gfp antibodies, respectively. Molecular weight standards are depicted on the left side of each of the panels.

Discussion

CENP-E–Kinetochore Interactions

To examine the molecular determinants that specify kinetochore binding by CENP-E, we identified its kinetochore targeting domain, and then used this to identify proteins that may mediate kinetochore binding by CENP-E. The kinetochore binding domain of CENP-E was found to lie within a 350–amino acid segment that is positioned near the COOH terminus but is separated from the COOH-terminal microtubule binding domain (Liao et al., 1994). The ability of this element to target heterologous proteins (either protein A or gfp) to the kinetochore defines this as a discrete functional domain that recognizes specific components at the kinetochore and establishes stable associations with them. Furthermore, the ability of the transfected kinetochore binding domain to displace endogenous CENP-E from kinetochores shows that this domain mediates interactions with kinetochore components that do not include CENP-E.

The identification of the kinetochore proteins CENP-F and hBUBR1 as proteins that associate with the kinetochore binding domain of CENP-E suggest that these proteins physically associate with each other at kinetochores. These three proteins can be distinguished from each other by the different times at which they assemble onto the kinetochore. CENP-F is first detected at the nascent kinetochores during late G2 when chromatin condensation is first apparent (Yen et al., 1992; Liao et al., 1994). By staining cells simultaneously with CENP-F and hBUBR1 anti-

bodies, we identified prophase cells whose kinetochores contained CENP-F but not hBUBR1. Thus, hBUBR1 must assemble onto the kinetochore shortly after CENP-F. The earliest time when hBUBR1 was detected at kinetochores was during prophase, after CENP-F is already bound to the nascent kinetochore. hBUBR1 assembly onto kinetochores was followed by the appearance of CENP-E shortly after nuclear envelope breakdown. As it was difficult to assess the integrity of the nuclear envelope of cells that are about to enter mitosis, we cannot tell whether hBUBR1 was selectively imported into prophase nuclei or diffused through perforations in the nuclear envelope.

While it was not a great surprise that a nuclear protein such as CENP-F would be recruited to kinetochores before cytoplasmic proteins, we did not expect hBUBR1 and CENP-E, both cytoplasmic proteins, to assemble onto kinetochores in sequential fashion. This suggests that hBUBR1 assembly onto kinetochores was unlikely to depend on CENP-E but perhaps on CENP-F and other proteins that were already assembled at the kinetochore. Once hBUBR1 was assembled at the kinetochore, its interactions with other kinetochore proteins might create a binding site for CENP-E. Taken together, these observations suggest that a highly ordered kinetochore assembly pathway exists whereby the proper assembly of one kinetochore component must occur before subsequent components can be added.

The combined data from yeast two-hybrid, coimmunoprecipitation, and cotransfection experiments show that CENP-E forms a stable complex with hBUBR1 in HeLa cells. We are currently testing whether hBUBR1 can directly bind CENP-E or if the interaction requires other proteins. Regardless of how these two proteins interact, using the same conditions that preserved the CENP-E–hBUBR1 complex, CENP-F was not found to form complexes with either CENP-E or hBUBR1 in HeLa lysates. The sequential order of appearance of CENP-F, hBUBR1, and CENP-E at the kinetochore indicates that these proteins do not assemble as a pre-formed complex. Once assembled onto the kinetochore, these proteins may establish associations with each other. The interaction between CENP-E and CENP-F maybe very similar in nature to that reported for the kinetochore protein hzw10 and dynamitin, a subunit of the dynactin complex. Dynamitin was identified in a hzw10 yeast two-hybrid screen. Yet, these two proteins failed to coimmunoprecipitate from cell lysates or bind in vitro. Nevertheless, genetic analysis of zw10 *Drosophila* mutants showed that the recruitment of dynein and dynactin to kinetochores required the presence of zw10 at kinetochores (Starr et al., 1998). Although we favor the interpretation that the CENP-E and CENP-F interaction that was detected by yeast two-hybrid reflect their interaction at the kinetochore, it remains possible that they also interact at other places in the cell where they colocalize such as the spindle midzone and the midbody (Liao et al., 1995; Cooke et al., 1997).

The Kinetochore Binding Domain of CENP-E Is Complex

Analysis of the minimal kinetochore binding domain by the COILS2 program (Lupas et al., 1991) show that a large segment of this region is predicted to form coiled-coil interactions. It remains to be seen whether this exists as a continuous or segmented coil. One of the coiled-coil interactions is likely to be CENP-E itself as yeast two-hybrid data that showed that the kinetochore binding domain of CENP-E can self-associate. That CENP-E can exist as a homodimer is supported by earlier findings that the mass of native CENP-E is ~850 kD (Thrower et al., 1996). In addition to CENP-E self-association, the kinetochore binding domain also associated with hBUBR1 in HeLa cells. Although the precise region of hBUBR1 that specifies CENP-E interactions have not been defined at a high resolution, the results presented here show that it lies within the COOH-terminal 641 amino acids. It is noteworthy that CENP-E did not associate with the NH_2-terminal portion of hBUBR1 that contained the highly conserved MAD3-like domain. It appears that hBUBR1 contains a CENP-E binding site that is not present in hBUB1 as we have not detected interactions between CENP-E and hBUB1 (Yen, T.J., unpublished observations).

Kinetochore Binding by CENP-E Is Temporally Regulated

Although CENP-E is only detected at kinetochores during mitosis, our data show that this may be due in part to a cell cycle–dependent phenomenon as the kinetochore binding domain of CENP-E failed to bind to interphase centromeres even when it was expressed in the nucleus. Although we cannot control the phase of the cell cycle in which to express the transfected protein, when CENP-F antibodies were used to selectively stain nuclei of cells that were in G2 (Liao et al., 1995), we found cells expressing the transfected CENP-E that were both positive and negative for CENP-F (data not shown). We are therefore reasonably sure that expression of the transfected construct occurred in most stages of interphase. The inability of the kinetochore binding domain to recognize centromeres during interphase is likely due to the absence of proteins that can stably bind CENP-E or the inappropriate cell cycle–specific modifications to such proteins. As the NLS-tagged CENP-E construct was associated with kinetochores of mitotic cells, it suggests that the ectopic nuclear localization did not interfere with kinetochore binding activity once the transfected cells entered mitosis. The notion that centromeres must undergo transitions during the cell cycle so that it becomes competent for kinetochore assembly is supported by the localization pattern of proteins such as topoisomerase IIα and CENP-F that accumulate at nascent kinetochores at late stages of S and G2, respectively (Liao et al., 1995; Rattner et al., 1996). Our finding that CENP-E will bind to kinetochores only at mitosis further strengthens this idea.

The accumulation of the NLS-tagged kinetochore binding domain of CENP-E at the periphery of nucleoli is rather curious as other portions of CENP-E or CENP-F that were fused to the NLS were uniformly distributed throughout the nuclei and were excluded from nucleoli (data not shown). The interaction between centromeres, ACA antigens, and nucleoli in mammalian cells have been reported (Manuelidis and Borden, 1988; Ochs and Press,

1992; Leger et al., 1994). In addition, CENP-C was found to bind the nucleolar protein, UBF (NOR-90) in vitro (Pluta et al., 1996). Although their significance is unclear, these observations support the idea that certain regions of the nucleoli might associate with the interphase centromere and some of these interactions might be recognized by the kinetochore binding domain of CENP-E. However, these associations do not appear to include the centromere domains that were defined by CENP-B, as colocalization with CENP-E was not evident.

hBUBR1 Functions

Studies of yeast BUB1, mouse BUB1 and hBUB1 show that these proteins are essential for cells to arrest in mitosis in the presence of spindle and kinetochore defects (Hoyt et al., 1991; Spencer and Hieter, 1992; Roberts et al., 1994; Wang and Burke, 1995; Pangilinan and Spencer, 1996; Wells and Murray, 1996; Taylor and McKeon, 1997; Cahill et al., 1998). Examination of the distribution of hBUBR1 show that it can be found at kinetochores from prophase to mid-anaphase. As with other checkpoint proteins, kinetochores of unaligned chromosomes exhibited stronger staining of hBUBR1 and CENP-E (Chen and Murray, 1996; Li and Benezra, 1996; Taylor and McKeon, 1997; Kallio et al., 1998; Waters et al., 1998). This observation, coupled with the fact that CENP-E and hBUBR1 kinase can form a stable complex in vivo, raises the possibility that this complex might participate in the checkpoint pathway. Indeed, our microinjection studies show that hBUBR1 is important for cells to arrest in mitosis in the face of defective kinetochore functions (Chan, G.K.T., and T.J. Yen, manuscript in preparation).

One of the currently held views on how the checkpoint determines whether kinetochores are aligned or not is that it recognizes biochemical changes within the kinetochore that are brought about by changes in kinetochore tension or microtubule attachments (Gorbsky and Ricketts, 1993; Nicklas et al., 1995; Li and Nicklas, 1997; Nicklas, 1997; Waters et al., 1998). Although the issue of whether the checkpoint monitors kinetochore tension or microtubule occupancy is unsettled, the fact that CENP-E is important for kinetochore–microtubule interactions (Schaar et al., 1997; Wood et al., 1997) suggests that it along with hBUBR1 can function as a mechanosensor at kinetochores. Indeed, genetic links between components of the spindle checkpoint and molecular motors have been established. In budding yeast, the kinesin-like gene CIN8 was shown to exhibit a synthetic lethal relationship with checkpoint genes BUB1, BUB3, and MAD2 (Geiser et al., 1997). In *Aspergillus nidulans*, viability of dynein and the kinesin-like protein, BIMC mutants depended on *sldA* and *sldB,* which are homologues of BUB1 and BUB3, respectively (Efimov and Morris, 1998).

In addition to its role in the mitotic checkpoint, hBUBR1 might also be important for kinetochore assembly by functioning as either a structural or regulatory protein. Because hBUBR1 assembles onto the kinetochore before CENP-E, it may phosphorylate specific kinetochore proteins so that the complex becomes competent to bind CENP-E. This view is consistent with our belief that interphase centromeres lack certain proteins or cell cycle–dependent modifications that are important for recognition by the kinetochore binding domain of CENP-E. hBUBR1 may also play other roles during late stages of mitosis when the majority of hBUBR1 is localized to the spindle midzone. It is interesting to note that hBUBR1 did not colocalize with CENP-E at the spindle midzone but was distributed in two broad patches that flanked a narrow stripe of CENP-E. This observation suggests that hBUBR1 does not always form a complex with CENP-E.

BUB1 Kinases Contain a Conserved MAD3-like Domain

The NH_2 terminus of yeast BUB1 was shown to share strong homologies with yeast MAD3 (Roberts et al., 1994). Remarkably, this domain in mammalian BUB1 kinases has also been highly conserved through evolution. Comparison of the sequences showed that NH_2 terminus of hBUBR1 and yeast BUB1 exhibited the most similarities with MAD3, which was closely followed by mouse and hBUB1. Although the biochemical function of MAD3 in checkpoint control is not well understood, it appears to function downstream of or lie parallel to BUB1, BUB3, MAD1, and MAD2 (Elledge, 1996; Rudner and Murray, 1996). The strong evolutionary conservation of the MAD3-like domain in hBUBR1 and hBUB1 suggests that this domain associates with an evolutionary conserved protein that may be part of the kinetochore or other conserved components of the checkpoint pathway. This is supported in part by the finding that the MAD3-like domain lies within the kinetochore targeting domain for hBUB1 (mBUB1) and hBUBR1. Furthermore, the human BUB3 homologue was found to associate with hBUBR1 and mBUB1 through this domain (Taylor et al., 1998). While it is clear that the components of the mitotic checkpoint pathway are highly conserved, it is unclear as to why mammalian cells express two different BUB1 kinases. One possibility is that as the kinetochore became increasingly more complex in both structure and functions, the complexity dictated the need for additional regulatory proteins. It is possible that hBUB1 and hBUBR1 monitor the activities of different kinetochore proteins and operate along parallel pathways that are essential for establishing a functional checkpoint. A detailed biochemical analysis of these two protein kinases should clarify their contribution to kinetochore function and checkpoint control.

The authors would like to sincerely thank J. Hittle for expert technical support; Drs. S. Jablonski and D. Gately for suggestions and comments; S. Jablonski for providing hBUB1 antibodies; Dr. E. Golemis, and J. Estojak for yeast two-hybrid advice and reagents.

This work was supported by United States Public Health Services grant GM44762; Leukemia Society Scholar's Award, core grant CA06927; and Council for Tobacco Research and an appropriation from the Commonwealth of Pennsylvania.

Received for publication 26 March 1998 and in revised form 23 July 1998.

References

Brenner, S., D. Pepper, M.W. Berns, E. Tan, and B.R. Brinkley. 1981. Kinetochore structure, duplication, and distribution in mammalian cells: Analysis by human autoantibodies from scleroderma patients. *J. Cell Biol.* 91:95–102.

Cahill, D.P., C. Lengauer, J. Yu, G.J. Riggins, J.K. Wilson, S.D. Markowitz, K.W. Kinzler, and B. Vogelstein. 1998. Mutations of mitotic checkpoint genes in human cancers. *Nature.* 392:300–303.

Chen, C., and H. Okayama. 1987. High-efficiency transformation of mammalian cells by plasmid DNA. *Mol. Cell. Biol.* 7:2745–2752.
Chen, R.H., J.C. Waters, E.D. Salmon, and A.W. Murray. 1996. Association of spindle assembly checkpoint component XMAD2 with unattached kinetochores. *Science.* 274:242–246.
Cooke, C.A., R.L. Bernat, and W.C. Earnshaw. 1990. CENP-B: A major human centromere protein located beneath the kinetochore. *J. Cell Biol.* 110:1475–1488.
Cooke, C.A., B. Schaar, T.J. Yen, and W.C. Earnshaw. 1997. Localization of CENP-E in the fibrous corona and outer plate of mammalian kinetochores from prometaphase through anaphase. *Chromosoma (Basel).* 106:446–455.
Echeverri, C.J., B.M. Paschal, K.T. Vaughan, and R.B. Vallee. 1996. Molecular characterization of the 50-kD subunit of dynactin reveals function for the complex in chromosome alignment and spindle organization during mitosis. *J. Cell Biol.* 132:617–633.
Efimov, V.P., and R.N. Morris. 1998. A screen for dynein synthetic lethals in *Aspergillus nidulans* identifies spindle assembly checkpoint genes and other genes involved in mitosis. *Genetics.* 149:101–116.
Elledge, S.J. 1996. Cell cycle checkpoints—preventing an identity crisis. *Science.* 274:1664–1672.
Estojak, J., R. Brent, and E.A. Golemis. 1995. Correlation of two-hybrid affinity data with in vitro measurements. *Mol. Cell. Biol.* 15:5820–5829.
Fischer-Fantuzzi, L., and C. Vesco. 1988. Cell-dependent efficiency of reiterated nuclear signals in a mutant simian virus 40 oncoprotein targeted to the nucleus. *Mol. Cell. Biol.* 8:5497–5503.
Geiser, J.R., E.J. Schott, T.J. Kingsbury, N.B. Cole, L.J. Totis, and M.A. Hoyt. 1997. *Saccharomyces cerevisiae* genes required in the absence of the CIN8-encoded spindle motor act in functionally diverse mitotic pathways. *Mol. Biol. Cell.* 8:1035–1050.
Gorbsky, G.J., and W.A. Ricketts. 1993. Differential expression of a phosphoepitope at the kinetochores of moving chromosomes. *J. Cell Biol.* 122:1311–1321.
Gyuris, J., E. Golemis, H. Chertkov, and R. Brent. 1993. Cdi1, a human G1 and S phase protein phosphatase that associates with Cdk2. *Cell.* 75:791–803.
Hanks, S.K., and T. Hunter. 1995. Protein kinases 6. The eukaryotic protein kinase superfamily: kinase (catalytic) domain structure and classification. *FASEB (Fed. Am. Soc. Exp. Biol.) J.* 8:576–596.
Hanks, S.K., and A.M. Quinn. 1991. Protein kinase catalytic domain sequence database: identification of conserved features of primary structure and classification of family members. *Methods Enzymol.* 200:38–62.
He, D., and B.R. Brinkley. 1996. Structure and dynamic organization of centromeres/prekinetochores in the nucleus of mammalian cells. *J. Cell Sci.* 109: 2693–2704.
He, D., C. Zeng, K. Woods, L. Zhong, D. Turner, R.K. Busch, B.R. Brinkley, and H. Busch. 1998. CENP-G: a new centromeric protein that is associated with the α-1 satellite DNA subfamily. *Chromosoma (Basel).* 107:189–197.
Heim, R., A.B. Cubitt, and R.Y. Tsien. 1995. Improved green fluorescence. *Nature*. 373:663–664.
Hoyt, A.M., L. Trotis, and B.T. Roberts. 1991. *S. cerevisiae* genes required for cell cycle arrest in response to loss of microtubule function. *Cell.* 79:449–458.
Jin, D.Y., F. Spencer, and K.Y. Jeang. 1998. Human T cell leukemia virus type I oncoprotein Tax targets the human mitotic checkpoint protein MAD1. *Cell.* 93:81–91.
Kallio, M., J. Weinstein, J.R. Daum, D.J. Burke, and G.J. Gorbsky. 1998. Mammalian p55CDC mediates the association of the spindle checkpoint protein MAD2 with the cyclosome/anaphase promoting complex and is involved in the regulation of anaphase onset and late mitotic events. *J. Cell Biol.* 141: 1393–1406.
Leger, I., M. Guilland, B. Krief, and G. Brugal. 1994. Interactive computer-assisted analysis of chromosome 1 colocalization with nucleoli. *Cytometry*. 16:313–321.
Li, R., and A.W. Murray. 1991. Feedback control of mitosis in budding yeast. *Cell.* 66:519–532.
Li, X., and R.B. Nicklas. 1997. Tension-sensitive kinetochore phosphorylation and the chromosome distribution checkpoint in praying mantid spermatocytes. *J. Cell Sci.* 110:537–545.
Li, Y., and R. Benezra. 1996. Identification of a human mitotic checkpoint gene: hsMAD2. *Science.* 274:246–248.
Liao, H., G. Li, and T.J. Yen. 1994. Mitotic regulation of microtubule cross-linking activity of CENP-E kinetochore protein. *Science*. 265:394–398.
Liao, H., R.J. Winkfein, G. Mack, J.B. Rattner, and T.Y. Yen. 1995. CENP-F is a protein of the nuclear matrix that assembles onto kinetochore at late G2 and is rapidly degraded after mitosis. *J. Cell Biol.* 130:507–518.
Lupas, A., M. Van Dyke, and J. Stock. 1991. Predicting coiled coils from protein sequences. *Science.* 252:1162–1164.
Manuelidis, L., and J. Borden. 1988. Reproducible compartmentalization of individual chromosome domains in human CNS cells revealed by *in situ* hybridization and three-dimensional reconstruction. *Chromosoma (Basel).* 96: 397–410.
McEwen, B.F., J.T. Arena, J. Frank, and C.L. Rieder. 1993. Structure of the colcemid-treated PtK1 kinetochore outer plate as determined by high voltage electron microscopic tomography. *J. Cell Biol.* 120:301–312.
Muro, Y., H. Masumoto, K. Yoda, N. Nozaki, M. Ohashi, and T. Okazaki. 1992. Centromere protein B assembles human centromeric α-satellite DNA at the 17-bp sequence, CENP-B box. *J. Cell Biol.* 116:585–596.
Nicklas, R.B. 1997. How cells get the right chromosomes. *Science*. 275:632–637.
Nicklas, R.B., S.C. Ward, and G.J. Gorbsky. 1995. Kinetochore chemistry is sensitive to tension and may link mitotic forces to a cell cycle checkpoint. *J. Cell Biol.* 130:929–939.
Ochs, R.L., and R.I. Press. 1992. Centromere autoantigens are associated with the nucleolus. *Exp. Cell Res.* 200:339–345.
Palmer, D.K., K. O'Day, M.H. Wener, B.S. Andrews, and R.L. Margolis. 1990. A 17-kD centromere protein (CENP-A) copurifies with nucleosome core particles and with histones. *J. Cell Biol.* 104:805–815.
Pangilinan, F., and F. Spencer. 1996. Abnormal kinetochore structure activates the spindle assembly checkpoint in budding yeast. *Mol. Biol. Cell.* 8:1195–1208.
Pfarr, C.M., M. Coue, P.M. Grissom, T.S. Hays, M.E. Porter, and J.R. McIntosh. 1990. Cytoplasmic dynein is localized to kinetochores during mitosis. *Nature.* 345:263–265.
Pluta, A.F., and W.C. Earnshaw. 1996. Specific interaction between human kinetochore protein CENP-C and a nucleolar transcriptional regulator. *J. Biol. Chem.* 271:18767–18774.
Pluta, A.F., A.M. Mackay, A.M. Ainsztein, I.G. Goldberg, and W.C. Earnshaw. 1995. The centromere: hub of chromosomal activities. *Science.* 270:1591–1594.
Rattner, J.B., A. Rao, M.J. Fritzler, D.W. Valencia, and T.J. Yen. 1993. CENP-F is a *ca 400 KDa* kinetochore protein that exhibits a cell-cycle dependent localization. *Cell Motil. Cytoskeleton.* 17:227–235.
Rattner, J.B., M.J. Hendzel, C.S. Furbee, M.T. Muller, and D.P. Bazett-Jones. 1996. Topoisomerase II α is associated with the mammalian centromere in a cell cycle- and species-specific manner and is required for proper centromere/kinetochore structure. *J. Cell Biol.* 134:1097–1107.
Rieder, C.L. 1982. The formation, structure, and composition of the mammalian kinetochore and kinetochore fiber. *Int. Rev. Cytol.* 79:1–58.
Roberts, R.T., K.A. Farr, and M.A. Hoyt. 1994. The *Saccharomyces cerevisiae* checkpoint gene BUB1 encodes a novel protein kinase. *Mol. Biol. Cell.* 14: 8282–8291.
Rudner, A.D., and A.W. Murray. 1996. The spindle assembly checkpoint. *Curr. Opin. Cell Biol.* 8:773–780.
Saitoh, H., J. Tomkiel, C.A. Cooke, H. Ratrie III, M. Maurer, N.F. Rothfield, and W.C. Earnshaw. 1992. CENP-C, an autoantigen in scleroderma, is a component of the human inner kinetochore plate. *Cell.* 70:115–125.
Schaar, B.T., G.K.T. Chan, P. Maddox, E.D. Salmon, and T.J. Yen. 1997. CENP-E function at kinetochores is essential for chromosome alignment. *J. Cell Biol.* 139:1373–1382.
Sheay, W., S. Nelson, I. Martin, T.H. Chu, S. Bhatia, and R. Dornburg. 1993. Downstream insertion of the adenovirus tripartite leader sequence enhances expression in universal eukaryote vectors. *Biotechniques.* 15:856–862.
Shelby, R.D., K.M. Hahn, and K.F. Sullivan. 1996. Dynamic elastic behavior of α-satellite DNA domains visualized in situ in living human cells. *J. Cell Biol.* 135:545–557.
Spencer, F., and P. Hieter. 1992. Centromere DNA mutations induce a mitotic delay in *Saccharomyces cerevisiae. Proc. Natl. Acad. Sci. USA*. 89:8908–8912.
Starr, D.A., B.C. Williams, Z. Li, B. Etemad-Moghadam, R.K. Dawe, and M.L. Goldberg. 1997. Conservation of the centromere/kinetochore protein ZW10. *J. Cell Biol.* 138:1289–1301.
Starr, D.A., B.C. Williams, T.S. Hays, and M.L. Goldberg. 1998. Zw10 helps recruit dynacting and dynein to the kinetochore. *J. Cell Biol.* In press.
Steuer, E., L.A. Wordeman, T.A. Schroer, and M.P. Sheetz. 1990. Localization of cytoplasmic dynein to mitotic spindles and kinetochores. *Nature.* 345:266–268.
Sugimoto, K., H. Yata, Y. Muro, and M. Himeno. 1994. Human centromere protein C (CENP-C) is a DNA-binding protein which possesses a novel DNA-binding motif. *J. Biochem. (Tokyo).* 116:877–881.
Sugimoto, K., K. Kuriyama, A. Shibata, and M. Himeno. 1997. Characterization of internal DNA-binding and C-terminal dimerization domains of human centromere/kinetochore autoantigen CENP-C in vitro: role of DNA-binding and self-associating activities in kinetochore organization. *Chromosome Res.* 5:132–141.
Sullivan, K.F., M. Hechenberger, and K. Masri. 1994. Human CENP-A contains a histone H3 related histone fold domain that is required for targeting to the centromere. *J. Cell Biol.* 127:581–592.
Taylor, S.S., and F. McKeon. 1997. Kinetochore localization of murine Bub1 is required for normal mitotic timing and checkpoint response to spindle damage. *Cell.* 89:727–735.
Taylor, S.S., E. Ha, and F. McKeon. 1998. The human homologue of Bub3 is required for kinetochore localization of BUB1 and a MAD3/Bub1-related kinase. *J. Cell Biol.* 142:1–11.
Thrower, D.A., M.A. Jordan, B.T. Schaar, T.J. Yen, and L. Wilson. 1995. Mitotic HeLa cells contain a CENP-E-associated minus end-directed microtubule motor. *EMBO (Eur. Mol. Biol. Organ.) J.* 14:918–926.
Wang, Y., and D.J. Burke. 1995. Checkpoint genes required to delay cell division in response to nocodazole respond to impaired kinetochore function in the yeast *Saccharomyces cerevisiae*. *Mol. Cell. Biol.* 15:6838–6844.
Waters, J.C., R.-H. Chen, A.W. Murray, and E.D. Salmon. 1998. Localization of Mad2 to kinetochores depends on microtubule attachment, not tension. *J. Cell Biol.* 140:1193–1206.
Wells, W.A., and A.W. Murray. 1996. Aberrantly segregating centromeres activate the spindle assembly checkpoint in budding yeast. *J. Cell Biol.* 133:75–

84.
Wood, K.W., R. Sakowicz, L.S. Goldstein, and D.W. Cleveland. 1997. CENP-E is a plus end-directed kinetochore motor required for metaphase chromosome alignment. *Cell.* 91:357–366.
Wordeman, L., and T.J. Mitchison. 1995. Identification and partial characterization of mitotic centromere-associated kinesin, a kinesin-related protein that associates with centromeres during mitosis. *J. Cell Biol.* 128:95–105.
Yang, C.H., J. Tomkiel, H. Saitoh, D.H. Johnson, and W.C. Earnshaw. 1996. Identification of overlapping DNA-binding and centromere-targeting domains in the human kinetochore protein CENP-C. *Mol. Cell. Biol*. 16:3576–3586.
Yao, X., K.L. Anderson, and D.W. Cleveland. 1997. The microtubule-dependent motor centromere-associated protein E (CENP- E) is an integral component of kinetochore corona fibers that link centromeres to spindle microtubules. *J. Cell Biol*. 139:435–447.
Yen, T.J., D.A. Compton, D. Wise, R.P. Zinkowski, B.R. Brinkley, W.C. Earnshaw, and D.W. Cleveland. 1991. CENP-E, a novel human centromere-associated protein required for progression from metaphase to anaphase. *EMBO (Eur. Mol. Biol. Organ.) J*. 10:1245–1254.
Yen, T.J., G. Li, B.T. Schaar, I. Szilak, and D.W. Cleveland. 1992. CENP-E is a putative kinetochore motor that accumulates just before mitosis. *Nature.* 359:536–539.